Received: 15 February 2024 | Revised: 29 March 2024 | Accepted: 4 April 2024

DOI: 10.1111/ppl.14310

SHORT COMMUNICATION

Physiologia Plantarum

Mutations of *PsPALM1a* and *PsPALM1b* associated with the *afila* phenotype in Pea

Zhuo Yuan[1,2] | Xiaoting Xie[1,2] | Mingli liu[1,3] | Yexin He[1] | Liangliang He[1,2]

[1]Key Laboratory of Tropical Plant Resources and Sustainable Use, State Key Laboratory of Plant Diversity and Specialty Crops, Xishuangbanna Tropical Botanical Garden, Chinese Academy of Sciences, Kunming, Yunnan Province, China

[2]University of Chinese Academy of Sciences, Beijing, China

[3]College of Life Science, Southwest Forestry University, Kunming, China

Correspondence
Liangliang He,
Email: heliangliang@xtbg.ac.cn

Funding information
Strategic Priority Research Programs of the Chinese Academy of Sciences, Grant/Award Number: XDA26030301; National Natural Science Foundation of China, Grant/Award Number: 32170839; CAS-Western Light 'Cross-Team Project-Key Laboratory Cooperative Research Project', Grant/Award Number: xbzg-zdsys-202016; Yunnan Revitalization Talent Support Program, Grant/Award Number: XDYC-QNRC-2022-0335; Yunnan Fundamental Research Project, Grant/Award Number: 202101AW070004

Edited by Y. Jiao

Abstract

Semi-leafless represents an advantageous plant architecture in pea breeding due to its ability to enhance resistance to lodging and potentially to powdery mildew. The introduction of semi-leafless pea varieties is considered a seminal advancement in pea breeding over the past half-century. The *afila* (*af*) mutation leads to the replacement of lateral leaflets by highly branched tendrils; combined with the semi-dwarfing *le* mutation, it forms the semi-leafless cultivated variety. In this study, we identified that mutations in two tandemly-arrayed genes encoding Cys(2)His(2) zinc finger transcription factors, *PsPALM1a* and *PsPALM1b*, were closely associated with the *afila* phenotype. These two genes may be deleted in the *af* mutant. In situ hybridization showed that both genes exhibit specific expression in early leaflet primordia. Furthermore, suppression of *PsPALM1a/PsPALM1b* resulted in a high frequency of conversion of lateral leaflets into tendrils. In conclusion, our study provides genetic evidence demonstrating that mutations in *PsPALM1a* and *PsPALM1b* are responsible for the *af* locus, contributing to a better understanding of compound leaf formation in peas and offering new insights for breeding applications related to *afila*.

1 | INTRODUCTION

Pea (*Pisum sativum L.*) is one of the major agricultural crops cultivated globally (Cheng, 2022), ranked fourth in terms of harvested area among legumes, following soybeans, common beans, and chickpeas (http://www.fao.org/faostat/). The yield of peas significantly lags behind that of other leguminous crops (Li et al., 2017). Altering the architectural features, such as improving lodging resistance, can simplify cultivation practices and significantly increase yield. Notably, genes involved in regulating leaf morphology play a crucial role in determining pea architecture.

Pea belongs to the inverted repeat-lacking clade (IRLC) of the legume family (LPWG, 2017) and exhibits unique leaf morphological characteristics (Marx et al., 1987). Classic leaf mutants identified in peas included *unifoliata* (*uni*) (Hofer et al., 1997), *tendril-less* (*tl*) (Hofer et al., 2009), *cochleata* (*coch*) (Couzigou et al., 2012), and *stipule reduced* (*st*) (Moreau et al., 2018). The genes responsible for these mutants have been cloned. However, *afila* (*af*), another important mutant, has not yet been cloned. The *af* mutant, firstly described in 1953 (Kujala et al., 1953), is characterized by the transformation of all leaflets into tendril branches, but retaining a normal pair of stipules. This semi-leafless feature has then been extensively used in modern pea breeding programs, giving rise to new varieties, such as Wasata, a semi-leafless pea variety developed in Poland in 1979 using gamma-ray mutagenesis (Solanki et al., 2011). Physiological and field studies have demonstrated the advantages of "semi-leafless" varieties over traditional leaf types, including improved standability and reduced canopy disease severity (Kof et al., 2004; Tran et al., 2022). Consequently, major pea-producing countries like France and Canada predominantly cultivate semi-leafless varieties.

The *af* mutation was located on linkage group (LG) I, chromosome 2 (Marx, 1969), near the locus *i* determining pea seed color (Ellis, 2002). Further studies involving crosses with other pea leaf mutants (Marx, 1987) and gene expression analysis have provided preliminary insights into the function of *AF* (Gourlay et al., 2000). *AF* has been identified as a negative regulator of *UNI* gene and auxin synthesis (Hofer & Ellis 1998; DeMason et al., 2013). Previous investigations have demonstrated that in two closely related legume species, *M. truncatula* and chickpea, the Cys(2)His(2)-zinc finger transcription factor *PALM1/MPL1* directly represses the *UNI* ortholog *SINGLE LEAFLET1* (*SGL1*) or *CaLFY*, maintaining the normal development of lateral leaflets (Chen et al., 2010; He et al., 2020; Liu et al., 2023). In the *palm1* and *mpl1* mutants, the complexity of the lateral region of leaves was significantly increased. Phylogenetic analysis showed that, in pea genome, two tandemly-arrayed *PALM1/MPL1* orthologs located on the end part of the chromosome Chr2LG1, which corresponded to the *AF* locus in the linkage group LGI. A recent preprint article speculated that deletion of the two *PALM1/MPL1* orthologs is likely responsible for the *af* phenotype (Tayeh et al., 2023). In our present study, we also found that mutations in the two genes, *PsPALM1a* and *PsPALM1b*, were closely associated with the *afila* phenotype, and these two genes may be deleted in the *af* mutant.

2 | MATERIALS AND METHODS

2.1 | Plant materials, growth conditions and statistical analysis

The pea line JI992 (provided by Dr. Mike Ambrose, John Innes Institute, UK) and the sequencing variety ZW6 were used as wild type (WT) plants. The *af* mutant line in the present study referred to the "Mawan1" variety previously described (Fu et al., 2016). The *tl* mutant line JI32 was also supplied by M. Ambrose, and the *af tl* line was created through a cross between Mawan1 and JI32. All materials were grown in a greenhouse under controlled conditions featuring a 16-hour light and 8-hour dark cycle, light intensity of 150 μmol/m^2/s, and temperature controlled at 18–23°C. The statistical analysis of the number of leaves, leaflets and tendrils at different nodes in both WT and *af* plants was conducted on five two-month-old plants for each genotype.

2.2 | Retrieval of gene sequences and phylogenetic analysis

Pea genome sequences were obtained directly from the "Pea Genome project" (https://urgi.versailles.inra.fr/Species/Pisum/Pea-Genome-project) for the "Cameor" genome (Kreplak et al., 2019) and from the latest version of the "ZW6" genome available in the "Pea Genome Database" (https://www.peagdb.com/) (Yang et al., 2022).

Phylogenetic analysis was conducted by retrieving PALM1 homologs from Phytozome (https://phytozome.jgi.doe.gov/pz/portal.html). Multiple alignments of PALM1 protein sequences were generated using ClustalX (v2.1) with default parameters and presented in Data S1. The maximum likelihood method was employed for phylogenetic analysis with IQTREE v1.6.10 using the JTT + F + G4 model recommended by the IQTREE model test tool (BIC criterion). Ultrafast bootstrap replicates of 2000 and iterations of 5000 were utilized to ensure statistical significance of the results. The resulting tree was edited using the MEGA 5.0 program.

2.3 | DNA extraction and polymerase chain reactions

DNA extraction from fresh leaves was performed using the 2x CTAB method. The primers (Table S1, designated as a ~ k) utilized for PCR to detect candidate genes and deletions at the *af* locus, were designed based on the "ZW6" reference genome. Visualization of the PCR products was achieved through agarose gel electrophoresis, followed by gel extraction and Sanger sequencing analysis.

2.4 | Virus-Induced Gene Silencing (VIGS) experiment

A 342-bp fragment from the 3′ end of the coding region of *PsPALM1a* was amplified using primers (Table S1) and cloned into pCAPE2 to construct the VIGS vector "PsPALM1a-PDS" (Constantin et al. 2004). Two agrobacterium GV3101 strains, one containing this construct and the other pCAPE1, were co-inoculated and injected into the leaves of 2-week-old pea plants (JI992). Photographs were taken of mature leaves at the 13th to 14th nodes of the VIGS-*PsPALM1a-PDS* and VIGS-*PsPDS* plants exhibiting bleaching symptoms. Subsequently, the frequency and types of leaflets and tendrils were recorded from 25 plant individuals for each experimental group. All VIGS experiments were replicated independently three times.

2.5 | RNA isolation, RT-qPCR, and data analysis

Total RNA was extracted from various tissues and leaf primordia of pea at different developmental stages using the RNA simple Total RNA Kit (DP419, Tiangen). cDNA was synthesized from 5 μg total RNA using the Superscript™ First-Strand Synthesis System (R212, Vazyme). RT-qPCR assays in pea were performed using the TransStart Tip Green qPCR SuperMix (AQ141, TransGen) on the Roche LightCycler480II platform, with *PsEF1a* used as the internal reference gene. The RT-qPCR primers are available in Table S1. The expression levels of target genes were determined using the $2^{-\Delta\Delta CT}$ method (Livak and Schmittgen, 2001).

2.6 | RNA in situ hybridization

In situ hybridization was performed as previously described (Coen et al., 1990; Liu et al., 2023; He et al., 2024) with minor modifications.

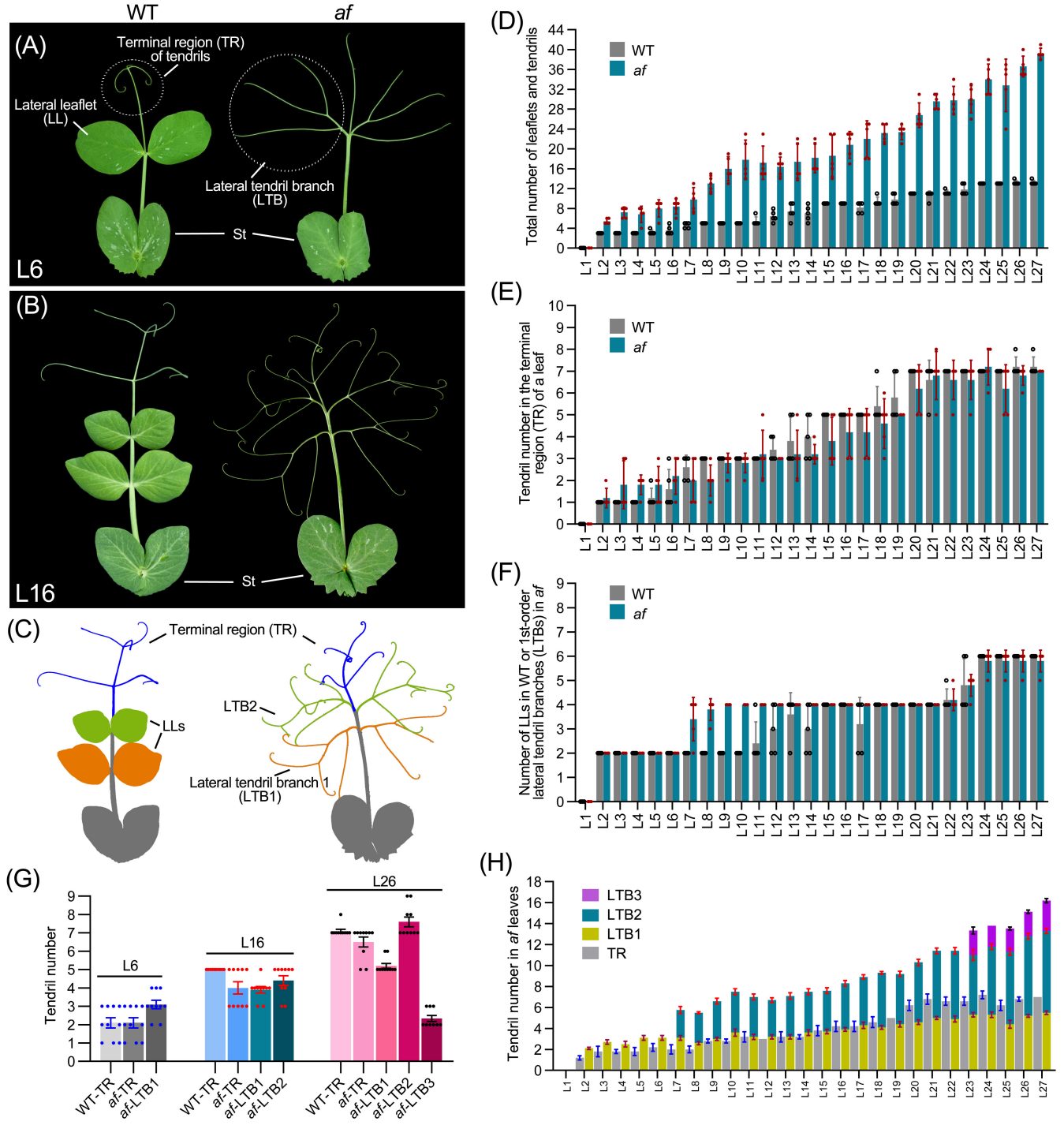

FIGURE 1 Phenotypic comparison of WT(JI992) and the *afila* (*af*, Mawan1) mutant of pea.
(A) Image comparison of compound leaves at the L6 node from WT and *af*.
(B) Image comparison of compound leaves at the L16 node from WT and *af*.
(C) Illustration of the compound leaf structures at the L16 node from WT and *af*.
(D) Quantification of total leaflet and tendril numbers in compound leaves from nodes L1–L27.
(E) Quantification of tendril numbers in the terminal region (TR) of leaves from nodes L1–L27.
(F) Quantification of lateral leaflet (LL) number in WT leaves or 1st-order lateral tendril branch (LTB) number in *af* leaves at nodes L1–L27.
(G) Comparison of tendril numbers between the terminal region (TR) of WT leaves and the TR and different LTBs of *af* leaves at representative nodes L6, L16, and L26.
(H) Quantification of the tendril number of different LTBs in *af* from nodes L1–L27.
Leaf nodes numbered from the cotyledon upwards; all data represent mean ± SD from 5 plants.

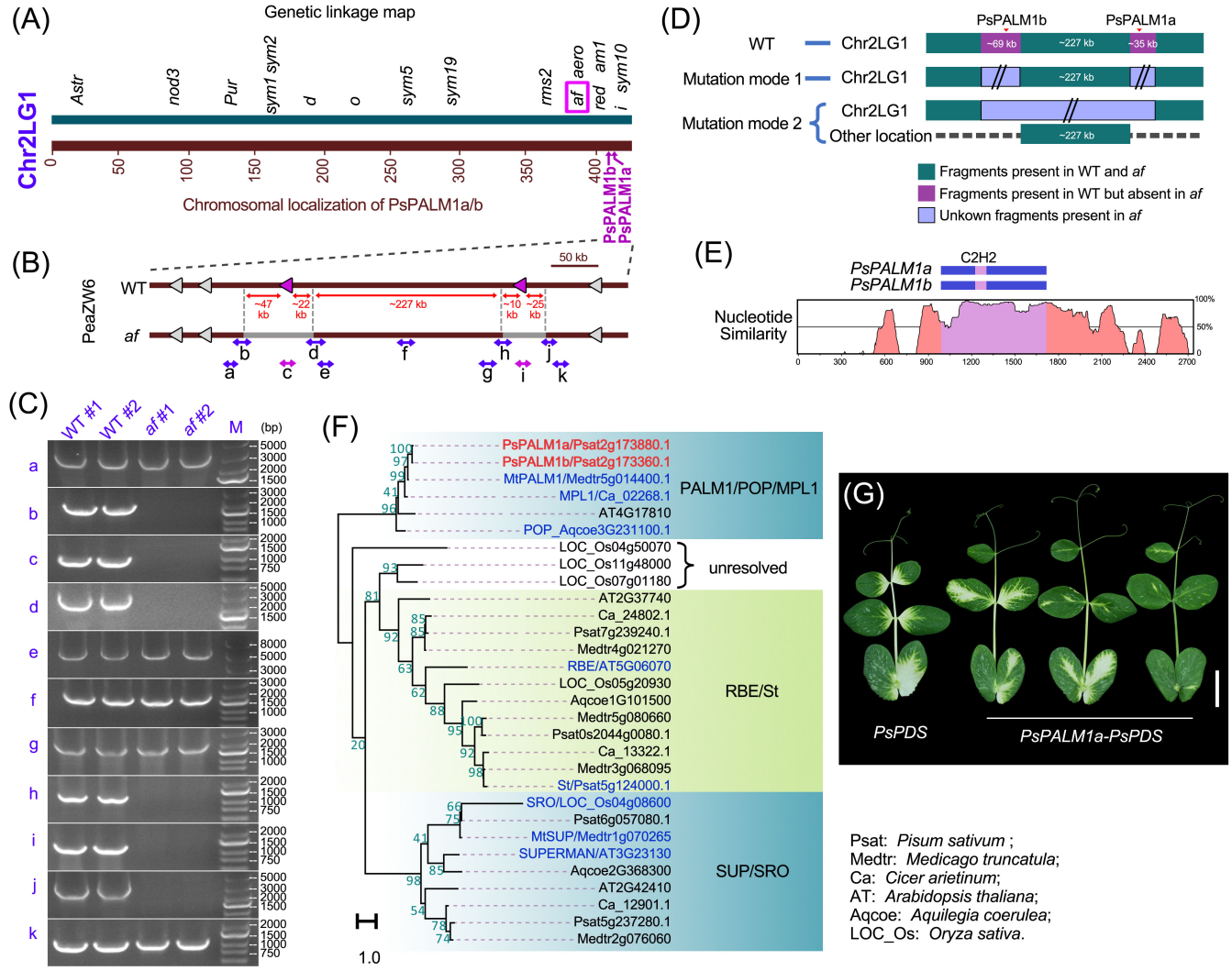

FIGURE 2 Molecular cloning and characterization of the *AF* candidate genes.
(A) Comparison of the *af* locus position on the genetic linkage map and the chromosomal localization of *PsPALM1a/b* in the pea genome version "PeaZW6".
(B) Schematic diagram illustrating the chromosomal organization of *PsPALM1a/b* and neighboring genes in the WT "PeaZW6" genome, as well as the corresponding chromosomal organization in the *af* genome. Each triangle represents an annotated gene, while gray lines indicate abnormal genomic fragments compared to WT. The letters a-k represent the genomic positions analyzed by PCR and sequencing.
(C) Agarose gel electrophoresis of PCR products (positions labeled in "B") in two WT plants and two independent *af* plants, with primer details provided in Table S1.
(D) Schematic diagram depicting possible genomic mutation modes at the *af* locus in the mutant genome.
(E) Schematic diagram showing the nucleotide similarity between *PsPALM1a* and *PsPALM1b*.
(F) Phylogeny of PsPALM1a, PsPALM1b and their homologs from other species, constructed using the maximum-likelihood method and bootstrap test with 2000 replicates. Numbers on nodes represent bootstrap values. Species abbreviations preceding the gene names are explained on the right side.
(G) Virus-induced gene silencing (VIGS) of *PsPALM1* in WT (JI992). Shown are representative leaves sampled from the L16 nodes of 2-month-old plants. Scale bar, 2 cm.

UNI, *PsPALM1a* and *PsPALM1b* probes against full-length complementary DNAs were used. Eight-micrometer sections from shoot apices of two-week-old seedlings were processed and hybridized with digoxigenin-labelled antisense probes. The signals were visualized with an Olympus BX63 microscope using differential interference contrast imaging.

3 | RESULTS AND DISCUSSION

Similar to other compound-leafed species, leaf development in pea also follows a pattern known as heteroblasty (Figures S1 and S2). In WT, after the cotyledons open, the first node develops small leaves known as "juvenile leaves". Starting from the second node upward,

compound leaves are formed, consisting of a pair of stipules at the base, 1–3 pairs of lateral leaflets (LLs), 0–2 pairs of lateral tendrils (LTs), and a terminal tendril (TT) (Figure S2). The complexity of these compound leaves gradually increases from the base to the apex of the plant (Figure S2).

Comparing the leaves of the *af* mutant with WT leaves, it is evident that, except for the normal basal stipules, the mutant leaves consist entirely of tendrils (Figures 1A, B, S1 and S2). When dissecting the *af* compound leaves into different regions, as shown in Figure 1C, it is observed that the terminal region (TR) of the mutant leaves resembles the tendril region in WT leaves; however, the LLs in the mutant are replaced by lateral tendril branches (LTBs). Statistical analysis reveals the following: (i) the number of tendrils in *af* leaves is significantly higher than the combined number of LLs and tendrils in WT leaves (Figure 1D), (ii) the number of tendrils in the TR of *af* leaves is not significantly different from the number of tendrils in WT leaves (Figure 1E), and (iii) the LTB number in *af* leaves is approximately equal to the number of LLs in WT leaves, with the exception of the 7th to 11th nodes, where the LTB number in *af* leaves usually exceed the LL number in WT leaves by one pair (Figure 1F). Further analysis shows that, in the same *af* leaf, the two most proximal pairs of LTBs exhibit a roughly equal number of tendrils to the number of tendrils in the TR (Figure 1G, H); however, for the *af* leaves containing three pairs of LTBs, the distal pair of LTBs shows a significant decrease in the number of tendrils (Figure 1G, H). Moreover, the epidermal cells of tendrils in the LTBs are identical to those of the TR tendrils (Figure S3).

These findings suggest that the *af* mutation transforms normal LLs into compound structures similar to the TR, while it does not significantly affect the TR structure.

The *AF* gene has already been mapped to the proximal end of Chr2LG1 (Figure 2A). Through collinearity and phylogenetic analysis, we identified two tandem-duplicated genes orthologous to the *PALM1* and *MPL1*, known as *PsPALM1a* (Psat2g173880) and *PsPALM1b* (Psat2g173360), located at the same chromosomal region (Figure 2B). In the reference genome version of the pea cultivar "Caméor", *PsPALM1a* and *PsPALM1b* are separated by 12 genes, totaling 521.5 kb (Figure S4). In the latest reference genome version "PeaZW6", *PsPALM1a* and *PsPALM1b* are not annotated as functional genes but are identified by Blast searching in the intergenic region, with *PsPALM1a* (chr2LG1 474041048–474041776) and *PsPALM1b* (Chr2LG1 473780760–473781479) separated by 259.6 kb (Figure 2B). The 12 genes separating *PsPALM1a* and *PsPALM1b* in the "Caméor" genome were also annotated in the "PeaZW6" genome, but positioned to the right of the *PsPALM1a* and *PsPALM1b* genes (Figure S4).

To determine whether *PsPALM1a* and *PsPALM1b* are candidate genes for the *af* mutation, we performed PCR analysis and Sanger sequencing of the regions surrounding these genes in both WT (ZW6) and the *af* mutant. The results showed that an approximately 35-kb-long fragment containing *PsPALM1a* and an approximately 69-kb fragment containing *PsPALM1b* were absent in the *af* mutant genome (Figure 2C). However, a sizable 227-kb fragment, located between these two fragments, was present in the *af* mutant genome (Figure 2C; gel images e, f and g). Due to the high sequence similarity between the boundaries of these abnormal fragments and other genomic regions and the presence of numerous SNP mutations, we have encountered difficulties in precisely defining their boundaries using conventional sequencing and tail-PCR. Therefore, we have proposed two possible mutation modes in the *af* mutant (Figure 2D). At first, the 35 kb and 69 kb fragments may be specifically replaced by other unknown fragments. Second, a 337 kb (35 + 227 + 69 kb) fragment, including both *PsPALM1a* and *PsPALM1b*, was replaced by an unknown fragment, while the large 227 kb fragment between *PsPALM1a* and *PsPALM1b* was relocated to another genomic location.

The coding sequences of *PsPALM1a* and *PsPALM1b* share a nucleotide similarity of 95% (Figure 2E). Phylogenetic analysis revealed that, as previously reported (Liu et al., 2023), PsPALM1a and PsPALM1b, together with PALM1, POP and MPL1, were tightly clustered and formed a distinct clade closely related to the SUPERMAN (SUP) and RABBIT EARS (RBE) clades (Figure 2F). Then, phenotypic analysis of VIGS-silenced plants revealed that the occurrence frequency of leaves having once leaflet-to-tendril transformation on a same leaf nodes was increased in the VIGS-*PsPDS-PsPALM1* plants compared to the VIGS-*PsPDS* plants, along with that the expression of *PsPALM1a* and *PsPALM1b* in vegetative shoots was decreased (Figures 2G and S5). These results indicate that the downregulation of *PsPALM1* can increase the transformation frequency of one of the most distal pairs of leaflets into a tendril in a leaf, suggesting that *PsPALM1a/b* play important roles in maintaining the leaflet characteristic.

The RT-qPCR analysis revealed that *PsPALM1a* and *PsPALM1b* displayed similar expression patterns in leaf-related tissues, with higher expression levels in vegetative shoots and lower expression levels in stipules (Figure 3A). Throughout leaf development, the expression of *PsPALM1a* and *PsPALM1b* was moderate during the stages of leaflet initiation (from SAM to P5), followed by an increase as leaves matured (from P6 to P8) (Figure 3B). Comparing the different tissues, the expression of *PsPALM1a* was consistently higher than that of *PsPALM1b* (Figure 3A,B). In situ hybridization further demonstrated that both *PsPALM1a* and *PsPALM1b* were detected in the lateral region of the compound leaf primordium (from which leaflet primordia were initiated) as well as leaflet primordia at different developmental stages (Figure 3C-G). However, their expression was weakly detected in stipule primordia, the tip region of the compound leaf primordium, and the initiating tendril primordia (Figure 3C, F and H). These data suggested that *PsPALM1a/b* expression occurs selectively in the proximal leaflet primordia (Figure 3I).

Previous studies suggested that the inverted repeat-lacking clade (IRLC) legumes rely on *LFY* orthologs to maintain the ability to initiate lateral leaflet and tendril primordia. *PALM1* and *MPL1* serve as key repressors of *LFY* expression, and their loss-of-function mutations led to *LFY* upregulation, thus increasing leaf complexity. Consistent with these findings, RT-qPCR revealed that significant upregulation of *UNI* (*PsLFY*) occurred in both vegetative shoot apices and leaf primordia of

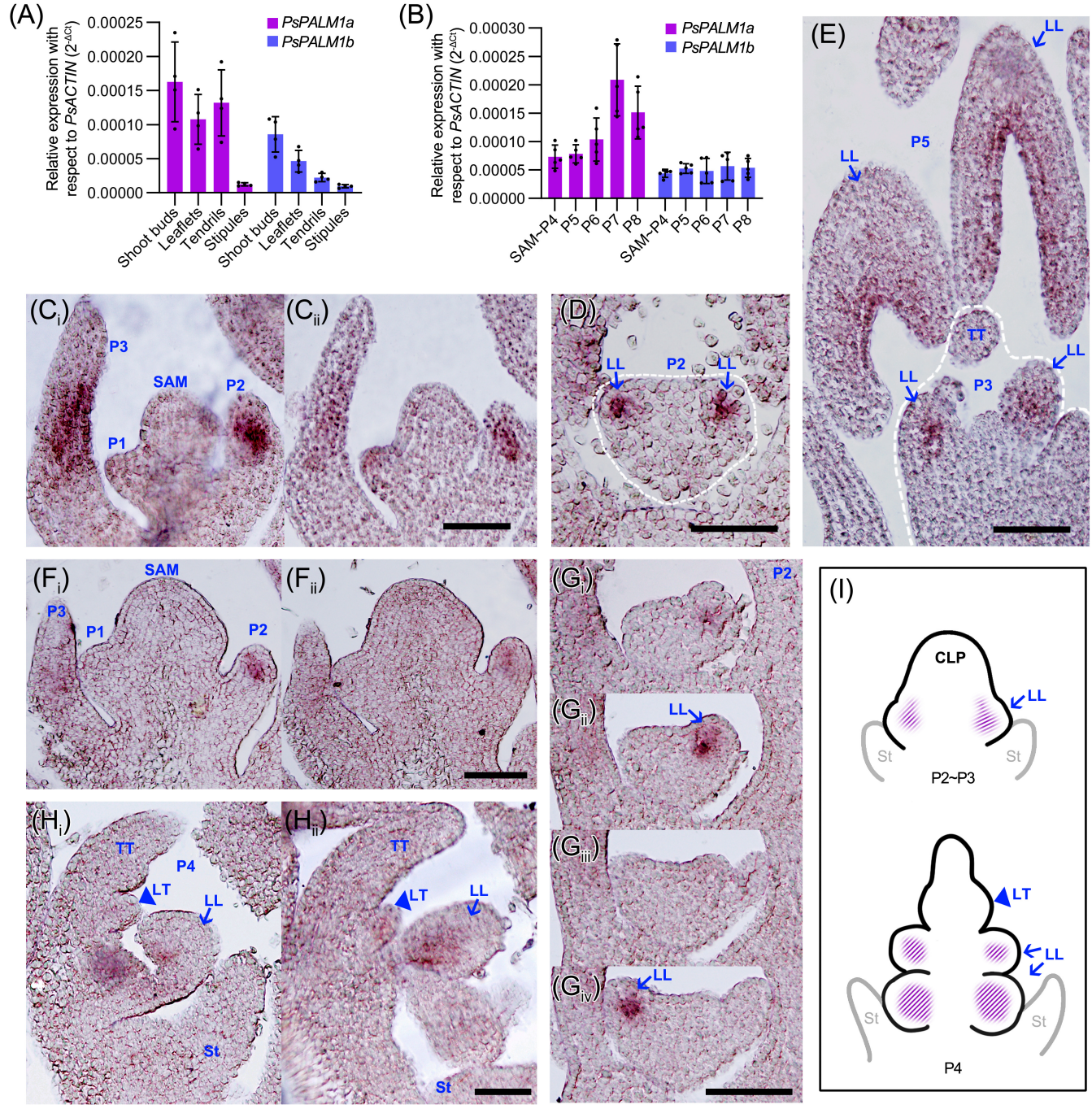

FIGURE 3 The spatio-temporal expression patterns of *PsPALM1a* and *PsPALM1b* during compound leaf development of pea.

(A) RT–qPCR analysis of *PsPALM1a* and *PsPALM1b* mRNA expression levels in different leaf-related tissues. Data shows mean ± SD of 4 biological replicates.

(B) RT–qPCR analysis of *PsPALM1a* and *PsPALM1b* mRNA expression levels at different leaf developmental stages. Data shows mean ± SD of 5 biological replicates.

(C-E) RNA in situ hybridization of *PsPALM1a*. Shown are serial longitudinal sections of a vegetative shoot (C), a cross-section of a P2 leaf primordium (D) and a longitudinal section of P5 and P3 leaf primordia (E) sampled from 2-week-old WT plants (JI992). Scale bars, 50 μm.

(F-H) RNA in situ hybridization of *PsPALM1b*. Shown are serial longitudinal sections of a vegetative shoot (F), serial cross-sections of a P2 leaf primordium (G) and a longitudinal section of P4 leaf primordium (H) sampled from 2-week-old WT plants (JI992). Scale bars, 50 μm.

(I) Diagrams of compound leaf primordia at P3 and P4 stages of ontogeny and the spatio-temporal expression pattern of *PsPALM1a/b* (purple). CLP, compound leaf primordium; LL, lateral leaflet; LT, lateral tendril; St, stipule. Blue arrows indicate leaflet primordia with clear in situ signals, and blue triangulars indicate initiating lateral tendril primordia.

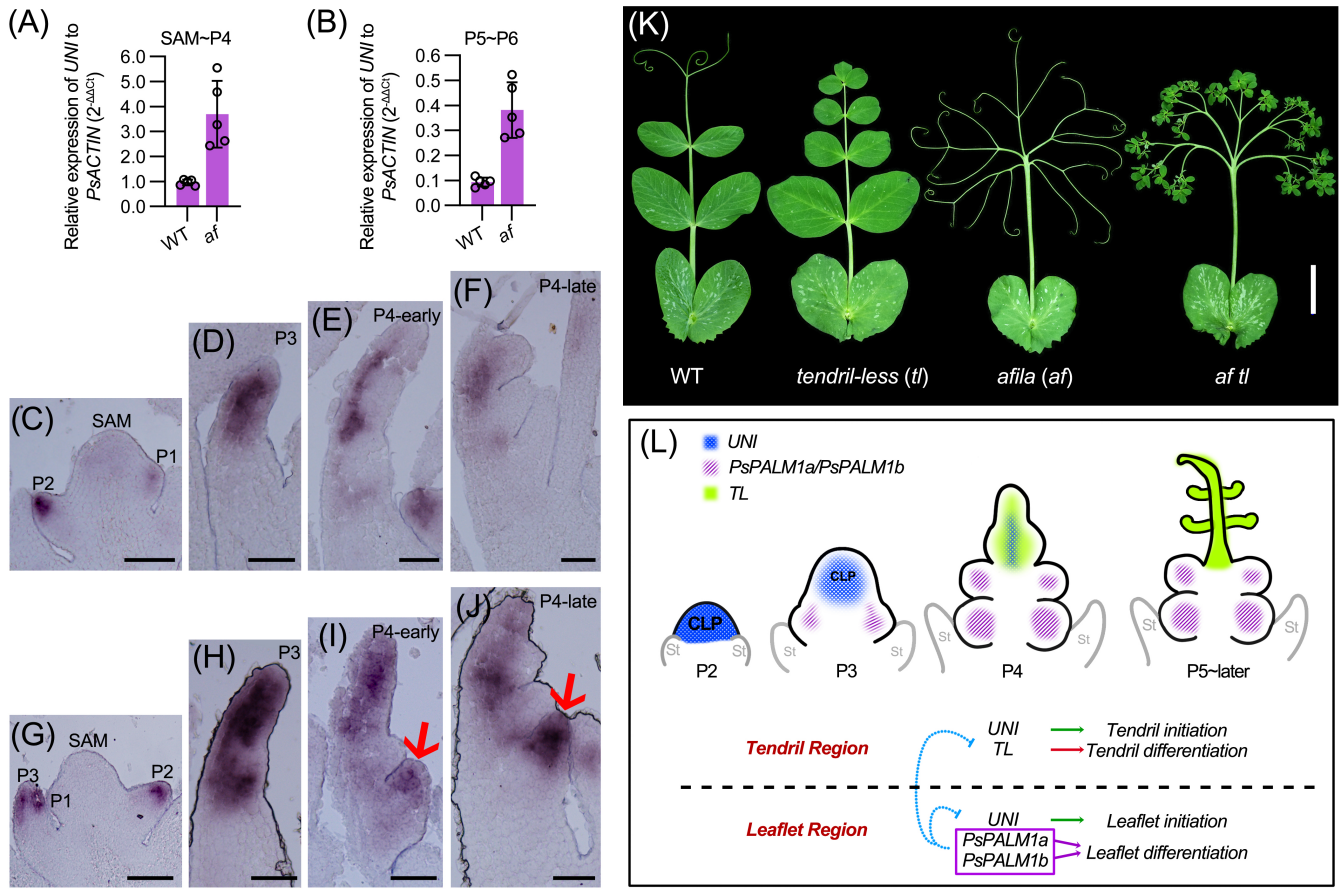

FIGURE 4 Molecular interactions among *AF*, *UNI* and *TL*.
(A-B) RT–qPCR analysis of *UNI* mRNA expression levels in the vegetative shoots (A) and P5 ∼ P6 leaf primordia (B) of WT and *af*. Data shows mean ± SD of 5 biological replicates.
(C-F) RNA in situ hybridization of *UNI* on longitudinal sections of vegetative shoots (C) and leaf primordia at different developmental stages (D-F) sampled from 2-week-old WT plants (JI992). Scale bars, 50 μm.
(G-J) RNA in situ hybridization of *UNI* on longitudinal sections of vegetative shoots (G) and leaf primordia at different developmental stages (H-J) sampled from 2-week-old *af* mutants. Red arrows indicate strong *UNI* signals detected in the proximal-initiating primordia of the early compound leaf primordium, which would develop into tendril branches during later stages. Scale bars, 50 μm.
(K) Genetic interaction of *af* with *tendril-less* (*tl*). Shown are representative leaves sampled from the L16 nodes of 2-month-old plants. Scale bar, 2 cm.
(K) A model for *UNI*, *TL* and *PsPALM1a/PsPALM1b* expression patterns and their interactions in P2, P3 and P4-P5 leaf primordia in WT.

the *af* mutants when compared to WT (Figure 4A,B). RNA in situ hybridization indicated that *UNI* was expressed in the tip of the early compound leaf primordium in WT, but weakly detected in the proximal region and the differentiated leaflet primordia (Figure 4C-F). In contrast, in the *af* mutant, strong *UNI* signals were also detected in the proximal-initiating primordia of the early compound leaf primordium (Figure 4G-J; red arrows), which would develop into tendril branches during later stages.

Based on the above results, we suggested that the loss-of-function of *PsPALM1a* and *PsPALM1b* is tightly linked to the phenotype of the *af* mutant. Combined with our recent study in chickpea (Liu et al., 2023), we propose that the PsPALM1a/PsPALM1b-UNI module and the chickpea MPL1-CaLFY module may have a similar role in regulating compound leaf morphogenesis. First, there is significant similarity in phenotype between the *af* mutant and *mpl1* mutant. In the *af* mutant, the proximal lateral leaflets transform into a complex structure of multiple tendrils, similar to those at the terminal region of the leaf, while in the *mpl1* mutant, the more proximal lateral leaflets transform into more complex structures with several leaflets, resembling the terminal region of a compound leaf. Second, similar to the complementary expression pattern of *MPL1* and *CaLFY* in chickpea compound leaf primordia, the expression patterns of *PsPALM1a* and *PsPALM1b* are also largely complementary to that of *UNI*. Both *mpl1* and *af* mutations lead to an upregulation of *LFY* ortholog expression. Therefore, it can be inferred that *PsPALM1a* and *PsPALM1b* are candidate genes for *AF*, regulating the expression of *UNI* to maintain the specific compound leaf pattern in peas. During pea compound leaf development, *UNI* is expressed at the undifferentiated tip of early compound leaf primordia, orderly initiating the leaflet primordia from the base to the tip. Once these leaflet primordia initiate, they immediately express *PsPALM1a* and *PsPALM1b* to suppress *UNI* expression, ensuring normal

development of the leaflet primordia. In the *af* mutant, the loss of *PsPALM1a* and *PsPALM1b* leads to the inability of leaflet primordia to suppress *UNI* expression, causing these leaflet primordia to acquire properties similar to those at the top of a compound leaf primordium, resulting in the formation of multiple tendril primordia.

Previous genetic pieces of evidence have revealed a complex interplay among *AF*, *UNI* and *TENDRIL-LESS* (*TL*) in determining the structure and composition of leaflets and tendrils in pea compound leaves (Figure 4K) (DeMason et al., 2001). The *TL* gene plays a specific role in determining tendril properties; in the *af tl* double mutant, all tendrils are transformed into leaflets (Figure 4K). Given that the downregulation of *PsPALM1a* and *PsPALM1b* through VIGS resulted in the conversion of some leaflets into tendrils (Figures 2G and S5) (Tayeh et al., 2023), it is reasonable to hypothesize that an ectopic expression of the *TL* gene may occur in the original leaflet primordia, leading to their transformation into tendril primordia. Thus, we proposed a possible mechanism underlying pea compound leaf structure determination (Figure 4L). *UNI* confers the potential for generating leaflet or tendril primordia for the whole compound leaf primordium. Early initiation of primordia from the basal region of the common compound leaf primordium is immediately followed by the expression of *PsPALM1a* and *PsPALM1b*, which cooperatively suppress *UNI* and potentially *TL*, thereby determining the properties of leaflet primordia at that position. Once all lateral leaflet primordia have completed initiation, the undifferentiated tip of the compound leaf primordium further generates new primordia, which promptly express *TL* but not *PsPALM1a* and *PsPALM1b*, thereby determining their properties as tendrils.

AUTHOR CONTRIBUTIONS

LLH conceived and designed the research. YZ performed the experiments. YZ and LLH drafted the manuscript. XXT, LML and YXH assisted with the experiments. All authors reviewed and approved the final manuscript.

ACKNOWLEDGMENTS

We thank Dr. Clarice Coyne (US Department of Agriculture-Agricultural Research Station Pacific West) and Dr. Mike Ambrose (The John Innes Centre) for providing the pea seeds and other assistance. This study was supported by National Natural Science Foundation of China (Grant No. 32170839), Strategic Priority Research Programs of the Chinese Academy of Sciences (Grant No. XDA26030301), CAS-Western Light 'Cross-Team Project-Key Laboratory Cooperative Research Project' (xbzg-zdsys-202016), Yunnan Revitalization Talent Support Program (Grant No. XDYC-QNRC-2022-0335) and Yunnan Fundamental Research Project (Grant No. 202101AW070004).

DATA AVAILABILITY STATEMENT

Data supporting the findings of this study are available within the paper.

ORCID

Liangliang He https://orcid.org/0000-0002-2169-4326

REFERENCES

Chen, J., Yu, J., Ge, L., Wang, H., Berbel, A., Liu, Y. et al. (2010). Control of dissected leaf morphology by a Cys (2) His (2) zinc finger transcription factor in the model legume *Medicago truncatula*. *Proceedings of the National Academy of Sciences*, 107(23), 10754–10759. https://doi.org/10.1073/pnas.1003954107

Cheng, S. (2022). Gregor Mendel: The father of genetics who opened a biological world full of wonders. *Molecular Plant*, 15(11), 1641–1645. https://doi.org/10.1016/j.molp.2022.10.013

Coen, E. S., Romero, J., Doyle, S., Elliott, R., Murphy, G., & Carpenter, R. (1990). *floricaula*: a homeotic gene required for flower development in *Antirrhinum majus*. *Cell*, 63(6), 1311–1322. https://doi.org/10.1016/0092-8674(90)90426-f

Constantin, G. D., Krath, B. N., MacFarlane, S. A., Nicolaisen, M., Elisabeth Johansen, I., & Lund, O. S. (2004). Virus-induced gene silencing as a tool for functional genomics in a legume species. *The Plant Journal*, 40(4), 622–631. https://doi.org/10.1111/j.1365-313X.2004.02233.x

Couzigou, J. M., Zhukov, V., Mondy, S., Abu el Heba, G., Cosson, V., Ellis, T. N et al. (2012). *NODULE ROOT* and *COCHLEATA* maintain nodule development and are legume orthologs of Arabidopsis *BLADE-ON-PETIOLE* genes. *The Plant Cell*, 24(11), 4498–4510. https://doi.org/10.1105/tpc.112.103747

DeMason, D. A., & J. Villani, P. (2001). Genetic control of leaf development in pea (*Pisum sativum*). *International Journal of Plant Sciences*, 162(3), 493–511. https://doi.org/10.1086/320137

DeMason, D. A., Chetty, V., Barkawi, L. S., Liu, X., & Cohen, J. D. (2013). *Unifoliata-Afila* interactions in pea leaf morphogenesis. *American journal of botany*, 100(3), 478–495. https://doi.org/10.3732/ajb.1200611

Ellis, T. H. N., & Poyser, S. J. (2002). An integrated and comparative view of pea genetic and cytogenetic maps. *New Phytologist*, 153(1), 17–25. https://doi.org/10.1046/j.0028-646X.2001.00302.x

Fu, J., Dong, L., Wang, F., Shen, S., Hou, G. (2016). Study on genetic characteristics of spotted gene in spotted colored pea. *Pratacultural Science*, 10(4): 655–661. https://doi.org/10.11829/j.issn.1001-0629.2015-0497 (in chinese)

Gourlay, C. W., Hofer, J. M., & Ellis, T. N. (2000). Pea compound leaf architecture is regulated by interactions among the genes *UNIFOLIATA*, *COCHLEATA*, *AFILA*, and *TENDRIL-LESS*. *The Plant Cell*, 12(8), 1279–1294. https://doi.org/10.1105/tpc.12.8.1279

He, L., Liu, Y., He, H., Liu, Y., Qi, J., Zhang, X et al. (2020). A molecular framework underlying the compound leaf pattern of *Medicago truncatula*. *Nature Plants*, 6(5), 511–521. https://doi.org/10.1038/s41477-020-0642-2

He, L., Liu, Y., Mao, Y., Wu, X., Zheng, X., Zhao, W et al. (2024) GRAS transcription factor PINNATE-LIKE PENTAFOLIATA2 controls compound leaf morphogenesis in *Medicago truncatula*, *The Plant Cell*, koae033, https://doi.org/10.1093/plcell/koae033

Hofer, J., Turner, L., Hellens, R., Ambrose, M., Matthews, P., Michael, A., & Ellis, N. (1997). *UNIFOLIATA* regulates leaf and flower morphogenesis in pea. *Current Biology*, 7(8), 581–587. https://doi.org/10.1016/S0960-9822(06)00257-0

Hofer, J. M., & Ellis, T. N. (1998). The genetic control of patterning in pea leaves. *Trends in Plant Science*, 3(11), 439–444. https://doi.org/10.1016/S1360-1385(98)01332-6

Hofer, J., Turner, L., Moreau, C., Ambrose, M., Isaac, P., Butcher, S et al. (2009). *Tendril-less* regulates tendril formation in pea leaves. *The Plant Cell*, 21(2), 420–428. https://doi.org/10.1105/tpc.108.064071

Kof, E. M., Oorzhak, A. S., Vinogradova, I. A., Kalibernaya, Z. V., Krendeleva, T. E., Kukarskikh, G. P et al. (2004). Leaf morphology, pigment complex, and productivity in wild-type and afila pea genotypes. *Russian Journal of Plant Physiology*, 51, 449–454. https://doi.org/10.1023/B:RUPP.0000035735.76190.6c

Kreplak, J., Madoui, M. A., Cápal, P., Novák, P., Labadie, K., Aubert, G et al. (2019). A reference genome for pea provides insight into legume genome evolution. *Nature genetics*, 51(9), 1411–1422. https://doi.org/10.1038/s41588-019-0480-1

Kujala, V. (1953). Felderbse bei welcher die ganze Blattspreite in Ranken umgewandelt ist. *Arch. Soc. Zool. Bot. Fenn*, 8, 44–45.

Legume Phylogeny Working Group (LPWG). (2017). A new subfamily classification of the Leguminosae based on a taxonomically comprehensive phylogeny. *taxon*, 66(1), 44–77. https://doi.org/10.5061/dryad.61pd6

Li, L., Yang, T., Liu, R., Redden, B., Maalouf, F., & Zong, X. (2017). Food legume production in China. *The Crop Journal*, 5(2), 115–126. https://doi.org/10.1016/j.cj.2016.06.001

Livak KJ, Schmittgen TD. (2001) Analysis of relative gene expression data using real-time quantitative PCR and the 2(-Delta Delta C(T)) method. *Methods* 25:402–408. https://doi.org/10.1006/meth.2001.1262

Liu, Y., Yang, Y., Wang, R., Liu, M., Ji, X., He, Y et al. (2023). Control of compound leaf patterning by *MULTI-PINNATE LEAF1* (*MPL1*) in chickpea. *Nature Communications*, 14(1), 8088. https://doi.org/10.1038/s41467-023-43975-9

Marx (1969) Linkage relations of *Af*. *Pisum Newsletter* 1:9–10

Marx, G. A. (1987). A suite of mutants that modify pattern formation in pea leaves. *Plant Mol. Biol. Rep*, 5(31), 1–335.

Moreau, C., Hofer, J. M., Eléouët, M., Sinjushin, A., Ambrose, M., Skøt, K et al. (2018). Identification of *Stipules reduced*, a leaf morphology gene in pea (*Pisum sativum*). *New Phytologist*, 220(1), 288–299. https://doi.org/10.1111/nph.15286

Solanki, R. K., Gill, R. K., Verma, P., & Singh, S. (2011). *Mutation breeding in pulses: an overview*. Breeding of pulse crops. Kalyani Publishers, Ludhiana, 85–103. https://doi.org/10.1002/9781118229415.ch1

Tayeh, N., Hofer, J., Aubert, G., Jacquin, F., Turner, L., Kreplak, J et al. (2023). *afila*, the origin and nature of a major innovation in the history of pea breeding. *bioRxiv*, [Preprint] Available from: https://doi.org/10.1101/2023.07.19.549624 [Accessed: 19th July 2023]

Tran, C. T., Becker, H. C., & Horneburg, B. (2022). Agronomic performance of normal-leafed and semi-leafless pea (*Pisum sativum* L.) genotypes. *Crop Science*, 62, 1430–1442.

Yang, T., Liu, R., Luo, Y., Hu, S., Wang, D., Wang, C et al. (2022). Improved pea reference genome and pan-genome highlight genomic features and evolutionary characteristics. *Nature genetics*, 54(10), 1553–1563. https://doi.org/10.1038/s41588-022-01172-2

SUPPORTING INFORMATION

Additional supporting information can be found online in the Supporting Information section at the end of this article.

How to cite this article: Yuan, Z., Xie, X., liu, M., He, Y. & He, L. (2024) Mutations of *PsPALM1a* and *PsPALM1b* associated with the *afila* phenotype in Pea. *Physiologia Plantarum*, 176(3), e14310. Available from: https://doi.org/10.1111/ppl.14310